www.amlett.com, www.amlett.org, DOI: 10.5185/amlett.2013.5477 Published online by the VBRI press in 2013

Green synthesis of gold nanoparticles for controlled delivery

S. Malathi[1], M. D. Balakumaran[2], P. T. Kalaichelvan[2], S. Balasubramanian[1*]

[1]*Department of Inorganic Chemistry, University of Madras, Chennai, India*
[2]*CAS in Botany, University of Madras, Chennai, India*

[*]Corresponding author. Tel: (+91) 9444016707; Fax: (+91) 4422300488; E-mail: bala2010@yahoo.com

Received: 19 May 2013, Revised: 29 June 2013 and Accepted: 01 July 2013

ABSTRACT

Gold nanoparticles (AuNPs) have been synthesized by green method using chitosan as a reducing/capping agent. We designed a biocompatible carrier for controlled release of hydrophobic drugs. The designed carrier was prepared by using single oil-in-water (O/W) emulsion. The resulting AuNPs were characterized by UV–Vis spectroscopy (UV–Vis) and Fourier transform infrared spectroscopy (FTIR). The transmission electron microscopy (TEM) studies indicate the spherical nature of drug loaded nanoparticles with the size of 50nm while the average particle size of AuNPs is found to be 2-3nm. The chitosan capped AuNPs showed a surface plasmon resonance at 526nm. The FTIR spectra suggest that the amine group is mainly responsible for the reduction of tetrachloroauric acid and capping the AuNPs. The controlled release of rifampicin (RIF) was investigated by *in vitro* studies using phosphate buffer saline (PBS) at pH=7.4. The loading efficiency of drug molecule was found to be 71%. The encapsulated drugs were released at 37 °C temperature. The results have been fit into various mechanistic models and it is found that the Higuchi model fits in to the release behavior of RIF. Further, the antibacterial activity of RIF loaded nanoparticles was examined by Gram +ve (*bacillus subtils*) and Gram -ve (*Pseudomonas aeruginosa*) bacteria. The application of similar drug loaded nanocarrier for treating other diseases like cancer can also be investigated. Copyright © 2013 VBRI press.

Keywords: Gold nanoparticles, chitosan, rifampicin, tuberculosis, drug delivery.

S. Malathi is a research scholar in the senior Department of Inorganic Chemistry, University of Madras. She has obtained her M.Phil degree in the same department. She has been working in the field of controlled drug delivery, polymer nanoparticles and metal nanoparticles. She has published her work in international journals and has participated in national and international conferences.

M. D. Balakumaran is a research scholar at Centre for Advanced Studies in Botany, University of Madras, Chennai. His major research area includes biomaterials, nanotechnology and their applications in the environmental and biomedical field.

P. T. Kalaichelvan is working as a Professor in Centre for Advanced Studies in Botany, University of Madras, Guindy Campus, Chennai, India. He has published several research papers in peer viewed national and international journals and conference proceedings. He has organized various conferences and workshops in the area of fermentation technology and nanomaterials. Under his able guidance more than 25 have completed their doctoral degree. His current area of research is focused on Nanobiotechnology, Enzyme technology, Microbial fuel cell, bioactive metabolites from plants and microbes.

S. Balasubramanian is a senior faculty in the Department of Inorganic Chemistry, Guindy campus, University of Madras, Chennai, India. He has more than 75 research publications in the field of macrocyclic complexes, macromolecular bound metal complexes, metal nanoparticles, biodegradable polymer nanoparticles for drug delivery. nanochemistry, environmental chemistry, leather chemistry and photochemistry. He is a fellow of the Royal Society of Chemistry, Commonwealth fellow in Oxford University and the Editor-in-Chief of Journal of Nanoscience Letters. He has travelled extensively and has delivered lectures in various universities around the globe.

Introduction

Advances in nanotechnology have identified promising candidates for many biological and biomedical applications not only for delivery of pharmaceutics, but also as novel diagnostics and therapeutic agents [**1-8**]. The small size of nanoparticles implies that they could get close to a biological target of interest. In the last decade, several delivery vehicles have been designed based on different nanomaterials, such as polymers [**9**], dendrimers [**10**], liposomes [**11**], nanotubes [**12**] and nanorods [**13**]. Gold nanoparticles (AuNPs) have recently emerged as attractive candidates for delivery into their targets [**14, 15**]. The payload could be small drug molecules or large biomolecules. There are several reasons for the use of AuNPs in nanotechnology. First of all, gold compounds have long been used in medicine through the history of civilization [**16**]. It is easy to synthesize AuNPs by several simple, economically cheap, safe and reliable technologies such as wet chemical, physical and biological methods [**17, 18**]. It can be synthesized in different shapes from 2-500 nm by changing the reaction parameters. Red-colored, antigen-modified gold nanoparticles allow diagnoses to be carried out rapidly and in straightforward manner both at home and in hospital, without the need for expensive equipment. When gold is employed for medical purposes as a drug, it is gold compounds rather than metallic gold nanoparticles that are used.

Among common ailments, *rheumatic diseases* are the major group associated with the clinical use of gold compounds, and in this respect several types of compounds, including sodium aurothiomalate, aurothioglucose and auranofin, have been developed and approved for clinical use [**19, 20**]. Several gold compounds have also been designed and tested as drugs to treat cancer, AIDS, bronchial asthma and malaria [**21**]. Among the various types of gold nanoparticles, the spherical form is the most widely used. As gold nanospheres can be easily prepared by reducing the gold ion and controlling the particle size, it is possible to carry out the production of gold nanoparticles with relative ease and subsequently to use them not only in a variety of medical diagnoses but also as therapeutic and drug delivery systems [**22**]. Due to the presence of negative charge on the surface of AuNPs, they are highly reactive, which helps to modify the surface of AuNPs using several biomolecules. It is well established that AuNPs are biocompatible and non-toxic [**23**].

Chitosan, a non-toxic biopolymer can be utilized to prepare precious metal nanocomposites [**24-32**] because it acts as dispersant and avoids metal particles agglomeration [**33-38**]. Bhumkar et al have reported chitosan stabilized gold nanoparticles as a carrier for transmucosal delivery of insulin [**39**]. Tuberculosis (TB) is the ubiquitous, highly contagious chronic granulomatous bacterial infection [**40**]. TB is the world's second most common cause of death from infectious disease, after acquired immunodeficiency syndrome (AIDS). Rifampicin (RIF) is a first-line drug for use in the list of recommended drug regimens for treatment of latent *Mycobacterium tuberculosis* infection in adults. A number of novel implants, microparticulates, and various other carrier – based drug delivery systems incorporating the principal antituberculosis agents have been fabricated that either target site of tuberculosis infection or reduce the dosing frequency with the aim of improving patient recovery. The fabrication of a chitosan capped gold nanoparticles which attains delivery of rifampicin for improved rifampicin bioavailability, could be a step in the right direction of treatment failure due to patient non-compliance.

In this report, green synthesis of chitosan stabilized AuNPs and drug loaded chitosan/Au nanoparticles and their characterization by various techniques such as UV–Vis, FTIR and TEM, will be described. The release kinetics and mechanism of rifmapicin as well as its antimicrobial activity will also be presented.

Experimental

Materials

Chloroauric acid (LR) ($HAuCl_4.xH_2O$,) (Loba Chemie, India), Chitosan (PG) (Sigma-Aldrich,USA) Rifampicin (Sigma-Aldrich, USA) were used without further purification. Dichloromethane (AR) (Fischer Scientific, India), Acetone (CG) (Qualigens, India) were used with further purification. Deionized water was used throughout the experiment. The *invitro* release measurement was carried out at pH 7.4 in PBS medium. Nutrient agar (LG) (Himedia, India) was used for microbiological tests. All other chemicals used were of reagent grade.

Green synthesis of AuNPs

Chitosan capped gold nanoparticles were prepared by the reduction of tetrachloroaurate with chitosan. 0.125M solution of $HAuCl_4.3H_2O$ was reduced by 100ml chitosan solution prepared in 0.5% acetic acid with vigorous stirring at 80˚C producing a ruby-red solution. Due to the poor solubility of chitosan, the mixture was kept overnight until a clear solution was obtained. Varying chitosan concentrations (0.1, 0.2, 0.3, 0.4 and 0.5%) were used for reduction of tetrachloroaurate to determine the effect of chitosan concentration on the formation of AuNPs.

RIF loading on AuNPs

Rifampicin (RIF) 5mg was dissolved in 5mL of DCM and chitosan capped AuNPs (chitosan/AuNPs) was dissolved in 2ml of deionized water. The drug solution was added to chitosan/AuNPs aqueous solution. The resultant oil-in-water (O/W) emulsion was sonicated using ultrasonicator (Hielscher, UP100H, Germany). Then the primary emulsion was stirred overnight for removing the solvent. The RIF encapsulated chitosan/AuNPs were harvested by centrifugation (C24, REMI centrifuge, India.) at 8,000rpm for 30min, washed thrice with distilled water. After final washing, nanoparticles were kept in a vacuum desiccator for 2days.

In vitro drug release studies

To determine the drug content, 2.5mg of RIF loaded chitosan/AuNPs were suspended in 2.5mL of DCM. The solution was stirred magnetically for 2h and the drug content was determined spectrophometrically. Absorbance of organic phase was measured at 475nm using UV–

Visible spectrophotometer (UV–Visible spectrophotometer, Perkin–Elmer ʎ35).

Drug content = [(Drug wt in RIF) – (chitosan/AuNPs) / (Total weight of RIF) – (chitosan/AuNPs)] × 100

Loading efficiency = [(Drug remaining in the nanoparticles) / (Feed weight)] × 100

The release of drugs from chitosan/AuNPs was investigated in a phosphate buffer solution (pH =7.4). The drug loaded nanoparticles (10mg) were immersed in 2 mL PBS buffer which was kept in a temperature controlled water bath. The release experiments were conducted at a controlled temperature (37°C). During the release, the sample was taken out at regular intervals and its absorbance was measured. The removed volume was replaced each time with 2 mL of fresh medium. The quantitative analysis of drug was based on UV–Visible data since the intensity of the peak ($ʎ_{max}$ 475nm) is dependent on the concentration of drug. The amount of released drug was determined after different time periods.

Determination of antimicrobial activity by well-diffusion method

The released RIF from chitosan capped gold nanoparticles were tested for antimicrobial activity by well-diffusion method against pathogenic organisms such as *Bacillus subtils* and *Pseudomonas aeruginosa* at different time intervals (3h, 6h, 12h and 24h). The pure cultures of organisms were subcultured on Muller-Hinton broth at 37°C on a rotary shaker at 200 rpm. Wells of 6-mm diameter were made on Muller-Hinton agar plates using gel borer. Each strain was swabbed uniformly onto the individual plates using sterile cotton swabs. Using a micropipette, 20µl (2.5mg/ml) of the sample of released drug solution was poured into each of four wells on all plates. After incubation at 37°C for 24 h, the plates were examined for evidence of zones of inhibition, which appear as a clear area around the wells. The diameter of such zones of inhibition was measured.

Characterizations

UV–visible spectroscopy (UV–Vis)

Absorption spectra of the synthesized chitosan stabilized AuNPs and rifampicin loaded chitosan/AuNPs composite solutions were recorded in aqueous and PBS medium using double-beam ʎ-35 spectrophotometer (Perkin–Elmer). The measurements were carried out using quartz cell in the wavelength range of 200-800nm.

Fourier infrared spectroscopy (FTIR)

FTIR of the synthesized chitosan stabilized AuNPs and rifampicin loaded chitosan/AuNPs composite were recorded using KBr pellets on a FTIR–Bruker Tensor 27, Fourier transform infrared spectrometer.

Transmission electron microscopy (TEM): TEM study was carried out on a FEI-TECHNAI, G2-MODEL (T-30 S-TWIN) transmission electron microscope with an acceleration voltage of 250kV. The samples for transmission electron microscope analysis were prepared by drop–coating chitosan/AuNPs, rifampicin loaded chitosan/AuNPs solution onto a copper grid and subsequent drying at room temperature.

Results and discussion

Generally gold nanoparticles are synthesized by using the various reducing agents such as sodium borohydride, trisodiumcitrate, thiocyanate, hydrazine, phosphorus, ascorbic acid, chitosan and even alcohols. Chitosan is the second most abundant polysaccharide in nature [**41-43**], and it can act as reducing agent as well as capping agent. In the present study, chitosan was used because of favorable biological properties such as low toxicity, and high susceptibility to biodegradation. It exhibits electronegative behavior and also acts as a polyelectrolyte electrostatic stabilizer. The amino group of the chitosan can act as a reducer as well as stabilizer (**Fig. 1**).

Five different concentrations (0.1%, 0.2%, 0.3%, 0.4% and 0.5%) of chitosan were employed for the NPs synthesis to establish the effect of the concentration of capping agent on the stability of the nanoparticles. The ruby red AuNPs with the capping agent (0.5% chitosan) was synthesized from a mixture of 0.5% chitosan in 0.5% acetic acid and 0.125M chloroaurate solution at 80˚C (**Scheme 1**). The protonation of amino group in chitosan occurs in acidic medium (R-NH_3^+) on the surface which provides a scaffold for the absorption of oppositely charged $AuCl_4^-$ ions.

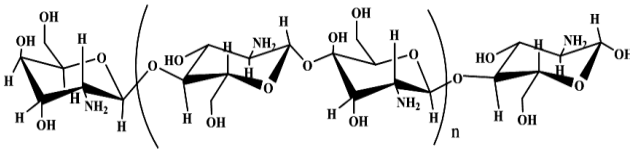

Fig. 1. Structure of chitosan.

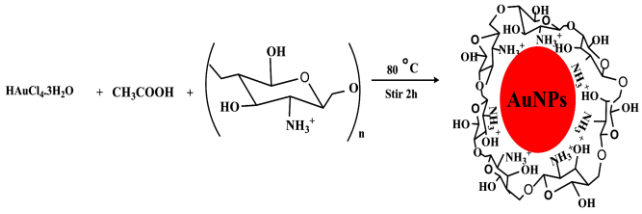

Scheme. 1. Schematic representation of synthesis of chitosan stabilized gold nanoparticles.

The electrostatic attractive forces between the positively charged amino group of chitosan and the negatively charged $AuCl_4^-$ ion drive the formation of nanoparticles and provide the nanoparticles high stability. After being reduced by the chitosan chain, the Au nuclei associated with AuNPs self assembled onto the surface of the chitosan as a result of both van der waals force and the high affinity between the amino group and the Au particles. The reaction temperature is also important for the size and shape of the nanomaterials. The complete reduction of AuNPs was observed within 10min at 80℃. The AuNPs with different concentration of the capping agent (0.1%, 0.2%, 0.3% and 0.4%) were synthesized under similar

condition. When the concentration of chitosan was increased, the color of the solution changes from pink to ruby red. The advantage of using chitosan for the reduction of chloroauric acid and the stabilization of as prepared AuNPs is that the method is easy and does not produce any environmental toxicity or biological hazards.

The formation of chitosan stabilized gold nanoparticles was confirmed by UV-Visible absorption spectroscopy. AuNPs solutions at different concentration of chitosan are shown in **Fig. 2**. The spectra exhibit a characteristic surface plasmon band of gold nanoparticles around 500-530nm [**44, 45**]. The position of the surface plasmon absorption band is sensitive to the metallic nanoparticle size, shape and spatial distribution.

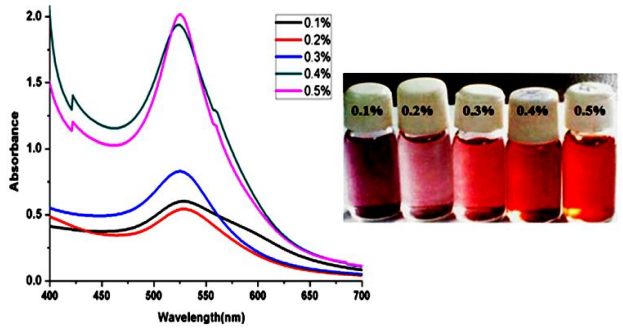

Fig. 2. UV-Visible absorption spectra of AuNPS prepared with different concentrations of chitosan. Inset: Photograph of the AuNPs at different concentrations.

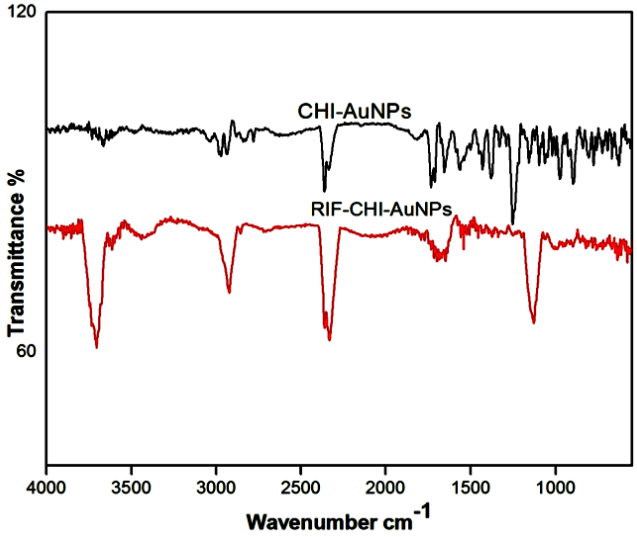

Fig. 3. FTIR spectra of a) CHI-AuNPs b) RIF-CHI-AuNPs.

Fig. 2 indicates UV–Vis spectra of chitosan stabilized AuNPs at different concentrations; it is evident from figure 1, with an increase in chitosan concentration, the surface plasmon band intensity also increases. The position of their absorption peaks are found to be 526nm (0.1%), 526nm (0.2%), 525nm (0.3%), 524nm (0.4%) and 525nm (0.5%) respectively. These results are consistent with previous reports on gold nanoparticles with chitosan as both reducing as well as capping agent [**46]**.It was observed that AuNPs form rapidly and the intensity of SPR band remained unchanged, without any shift in the peak wavelength even after 24h reduction time. Newman [**47**] has demonstrated that the distinct absorption peak of gold undergoes a red shift as the diameter of gold particle is increased.

The FTIR spectra of chitosan/AuNPs and RIF-chitosan/AuNPs are reproduced in **Fig. 3.** The former exhibits a peak at 1700cm^{-1} which is attributed to the C=O stretching frequency, and NH symmetric stretching is observed at 3550cm^{-1} while asymmetric and symmetric bending vibrations are observed at 1575cm^{-1} and 1440cm^{-1} respectively [**48**].

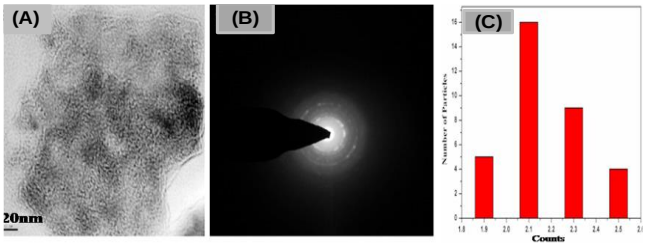

Fig. 4. TEM images of (A) AuNPs synthesized using chitosan at 0.5% concentration. (B) Selected area pattern of the dispersed phase (C) The histogram of the AuNPs.

TEM has been extensively used to investigate the morphology, size and selected area diffraction (SAED) of the synthesized AuNPs. The typical TEM image of AuNPs synthesized by reduction 0.125 M $HAuCl_4$ with a 5mg/ml chitosan solution is shown of **Fig. 4**. The uniform spherical shaped AuNPs is shown in **Fig. 4(A)** and the SAED pattern with spots is shown in **Fig. 4(B)**, each spot corresponding to a diffraction pattern of the crystalline gold structure. **Fig. 4(C)** represents histogram of AuNPs with particle size distribution the mean particle size of 2-3nm.

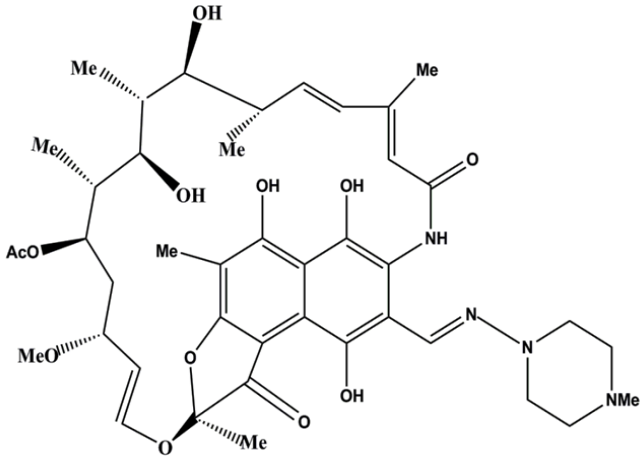

Fig. 5. Molecular structure of rifampicin.

Drug delivery

The efficacy of chitosan stabilized AuNPs for the controlled delivery of bioactive molecule has been investigated. The electrostatic interaction of the drug molecule plays a vital role in the controlled drug delivery. In the present investigation, first-line anti-TB drug rifampicin has been employed as a model drug (**Fig. 5**). The RIF loaded chitosan stabilized AuNPs were prepared by single oil-in-water (O/W) emulsion method (**Scheme 2**).

The physical interaction of hydroquinone group of rifampicin with chitosan stabilized gold has been postulated. Santos et al have reported that the interaction of rifampicin with chitosan is strongly dependent on pH [49]. The rifampicin is strongly adsorbed by chitosan at pH less than the pKa of the drug, and hence, chitosan can be an efficient carrier for the controlled release of rifampicin in the intestinal tract.

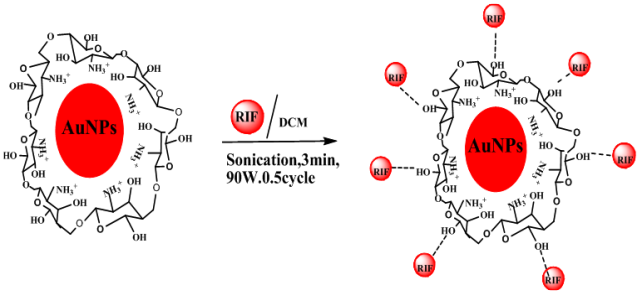

Scheme. 2. Schematic representation of synthesis of rifampicin loaded chitosan stabilized gold nanoparticles.

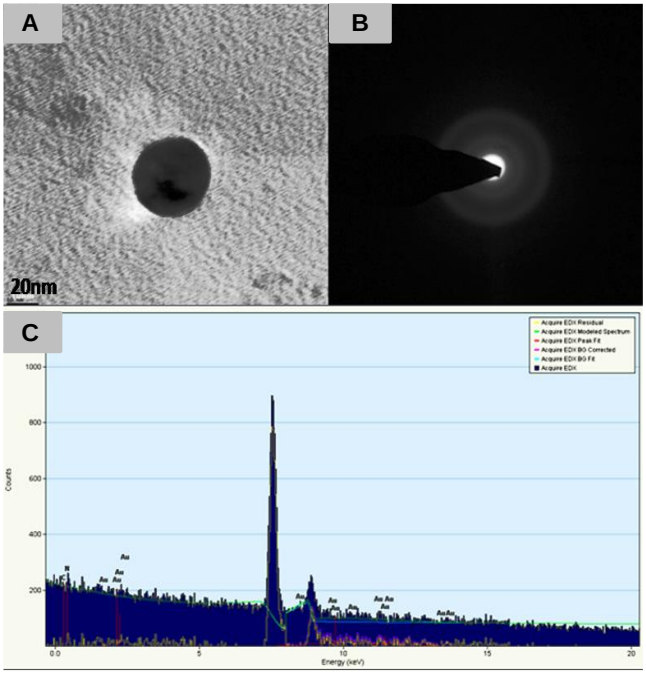

Fig. 6. a) TEM images of rifampicin encapsulated chitosan/Au nanocomposite. b) Selected area diffraction pattern c) The EDAX spectrum of the rifampicin encapsulated chitosan/Au nanocomposite.

The rifampicin in organic phase was added drop wise to chitosan stabilized AuNPs (water phase). Sonication time was optimized in order to achieve stable formulation with minimum average particle size and maximum loading efficiency. A stable nanoparticle formulation was achieved after sonicating the formulation for 5 min (30 kHz; 0.8cycle) with minimum average particle size and maximum loading efficiency i.e. 50nm and 71% respectively. The rifampicin loaded chitosan/AuNPs was stored at -4 ℃ for further studies.

The FTIR spectrum of RIF loaded chitosan/AuNPs exhibits the CH stretching frequency at 3050 cm^{-1} and CH bending frequency at 2450 cm^{-1}. The rifampicin loaded chitosan/AuNPs composite exhibits a distinct increase in the intensity of the peak at 3600cm^{-1} due to the OH stretching frequency of rifampicin drug molecule.

The TEM image of **Fig. 6(A)** shows the RIF loaded chitosan/AuNPs indicate its spherical nature. **Fig. 6(B)** shows the SAED pattern of RIF loaded Chitosan/AuNPs. The average particle size is found to be 50nm and all the particles are spherical in nature. The EDAX spectrum of RIF loaded chitosan/AuNPs (**Fig. 6(C)**) confirm that the observed particles were truly gold combined with drug. To determine drug concentration in the particles, an indirect method (UV–Visible) was used to calculate the loading efficiency in which, 5mg of nanoparticles was suspended in a small volume of DCM. The resulting solution was analyzed by UV–Visible spectrophotometer.

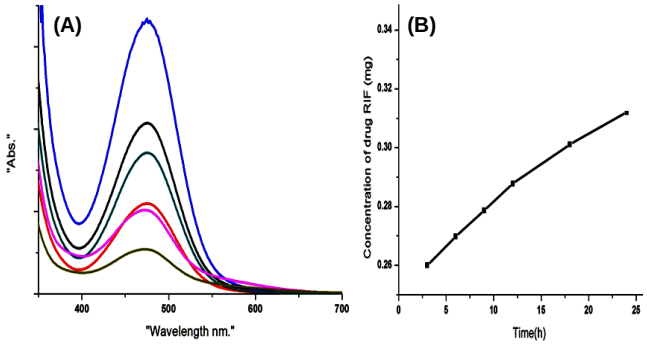

Fig. 7. (A) UV-Vis spectrum of RIF drug release (B) *In vitro* RIF drug release profile.

The loading efficiency of RIF on chitosan stabilized AuNPs was found to be 71%. The nature of binding of RIF to the chitosan/AuNPs plays vital role in the release and subsequent activity.

Chitosan significantly improved the drug loading efficiency of the nanoparticles due to the stronger electrostatic interaction between rifampicin and chitosan/Au nanoparticles. The amount of rifampicin released was calculated by UV–visible spectrophotometry at different time intervals (**Fig. 7(A)**). The released rifampicin was measured at 475nm. Similarly, from the UV–Visible spectral studies, the in vitro release profiles of the RIF loaded chitosan stabilized AuNPs showed a sustained release (**Fig. 7(B)**).

Drug release kinetics

The methods of approach to investigate the kinetics of drug release formulations are zero order, first order, Higuchi model, Korsmeyer–Peppas model etc.

Zero-order model

This model is applicable when the drug rate from polymer matrix is slow. In vitro drug release studies were plotted as cumulative amount of drug released Vs time. This relationship can be used for poorly soluble drugs.

$Q = k_0 t$

where, Q: Cumulative amount of controlled drug release at time t, K_0: Zero-order release constant. Zero-order: R^2 = 0.9703.

First order model

This model used to describe absorption or elimination of some drugs although it is difficult to understand the mechanism on theoretical basis. The first-order kinetics can be expressed by the following equation. In vitro kinetics was plotted as log cumulative percentage of drug release Vs time. It is useful to determine water-soluble drugs in porous matrices.

$$\ln Q = \ln Q_0 - Kt$$

where, Q_0: Initial concentration of drug, K: First-order rate constant, First-order: $R^2 = 0.9894$.

Higuchi model

Higuchi model is represented by the following equation. The model, which describes the release of drug from insoluble matrix as a square root of time, is a concentration dependent process based on fickian diffusion

$$Q = K_H t^{1/2}$$

where, K_H : Higuchi constant, Higuchi model: $R^2 = 0.9953$.

Korsmeyer–Peppas model

The mechanism of drug release, first 60% drug release were fitted in Korsmeyer–Peppas model

$$Mt / M\infty = Kt^n$$

where, $Mt / M\infty$: Fraction of drug release at time t, K: The release rate constant, n: release exponent. *In vitro* studies were plotted as log cumulative percentage of drug release Vs time.

Korsmeyar-Peppas model: R^2 =0.8062; n = 1.085.

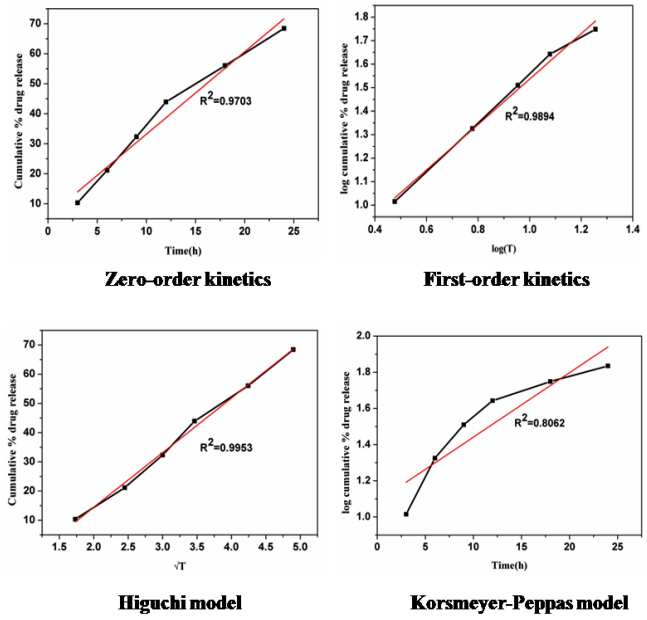

Fig. 8. Drug release kinetics of RIF loaded chitosan/Au nanocomposite.

The drug release data were fitted to those models which have been employed to establish the kinetics and release mechanisms. The four models that are commonly applied to drug release data from solid dosage forms are employed in the present investigation. The structure and geometry of the polymer network are important in the drug release. The mechanism of drug release from a chitosan /Au nanoparticles is diffusion-controlled and best fit is obtained with Higuchi model (**Fig. 8**) indicating distribution of RIF over the nanoparticles. The release of drug from the NPs depends on the characteristic of chitosan /AuNPs. When the nanoparticle is kept in the aqueous medium, water starts diffusing into the NPs thereby hydrating the same. The hydration of the composite starts at the surface and continues towards the center of the core. The release of RIF is dependent on the diffusion of water into the nanoparticles followed by the dissolution of the RIF and finally the diffusion of the dissolved RIF from the nanoparticles.

Antimicrobial studies

RIF is a well known broad spectrum antibiotic and it is typically used in the treatment of tuberculosis [**50**]. It is less active against gram-negative bacteria like E.Coli and Pseudomonas species. Since the nanoparticles can penetrate the bacterial cell wall more efficiently, the RIF-loaded nanoparticles will be more effective than free RIF. The antibacterial activities of RIF-loaded nanoparticles are shown in **Fig. 9**. It can be seen that RIF loaded chitosan stabilized AuNPs possess antibacterial activity against gram positive bacteria (*bacillus subtilis*) and gram negative bacteria (*Pseudomonas aerugionsa*).

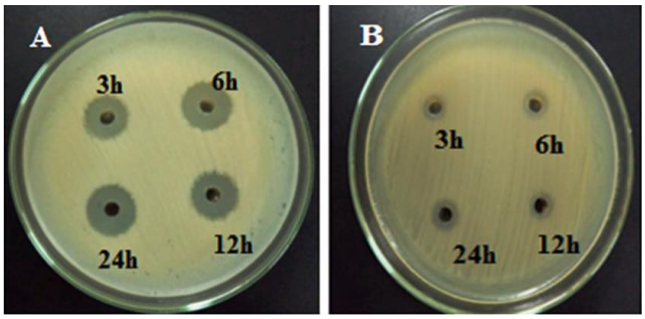

Fig. 9. Antibacterial studies of A) *Bacillus subtils* (Gram- positive) B) *Pseudomonas* aeruginosa (Gram- negative).

Conclusion

The green synthesis of AuNPs with chitosan as a capping as well as reducing agent has been reported. These nanoparticles exhibit a surface plasmon resonance at 526nm. Further, the applicability of these nanoparticles as a carrier for the delivery of anti tuberculosis drug has been demonstrated. A novel approach for the preparation of RIF loaded chitosan stabilized AuNPs is proposed by applying single O/W emulsion method. The synthesis, characterization, *invitro* release, and antibacterial activity of the NPs were investigated. The average particle size of chitosan/AuNPs and RIF loaded chitosan/AuNPs from TEM images are 2-3nm and 50nm respectively. The RIF loaded AuNPs are stable for prolonged storage and the nanospheres can be formulated for sustained release. The

drug release from the chitosan/AuNPs follows Higuchi model release kinetics. These attributes make RIF loaded AuNPs ideal for long term treatment and for improving drug compliance during the treatment of mycobacterium infections.

Acknowledgements

The authors would like to thank National center for nanoscience and nanotechnology (NCNST), University of Madras for carrying out HRTEM studies. The financial support by the Indian Council of Medical Research (ICMR), New Delhi is gratefully acknowledged.

Reference

1. Zhang, L.; Gu, F. X.; Chan, J. M.; Wang, A. Z.; Langer.; Farokhzad, O. C. *Clin. Pharmacol.Ther.* **2008**, *83*, 761. **DOI:** 10.1038/sj.clpt.6100400
2. Wang, L.; O'Donoghue, M. B.; Tan, W. *Nanomedicine(Lond)*, **2006**, *1*, 413. **DOI:** 10.2217/17435889.1.4.413
3. Ferrari, M. *Nature. Rev., Cancer.* **2005**, *5*, 161. **DOI:** 10.1038/nrc1566
4. Tiwari, A.; Tiwari, A. (Eds); *Nanomaterials in Drug Delivery, Imaging and Tissue Engineering*, Wiley-Scrivener Publishing, LLC, USA, **2013.** **DOI:** 10.1002/9781118644591
5. Tiwari, A.; Mishra, A. K.; Kobayashi, H.; Turner, A. P. F. (Eds); *Intelligent Nanomaterials, Processes, Properties and Applications*, Wiley-Scrivener Publishing, LLC, USA, **2012**. **DOI:** 10.1002/9781118311974
6. Ge,Y.; Tiwari, A.; Li, S. *Adv.Mat.Lett*. **2011**, 2, 1. **DOI:** 10.5185/amlett.2011.3001
7. Tiwari, A.; Prabaharan, M. *J. Biomater. Sci. Polym Ed.*, **2010**, 21, 937. **DOI:** 10.1163/156856209X452278
8. Parlak, O.; Tiwari, A.; Turner, A. P. F.; Tiwari, A.; *Biosens. Bioelectron*. **2013**, 49, 53. **DOI:** 10.1016/j.bios.2013.04.004
   Patra, H.K.; Khaliq, N.U.; Romu, T.; Wiechec, E.; Borga, M.; Turner, A.P.F.; Tiwari, A. *Advanced Healthcare Materials*, Published Online, **2013**. **DOI:** 10.1002/adhm.201300225
9. Malathi, S.; Balasubramanian, S. *J.Biomed.Nanotechnol*, **2011**, 7, **DOI:** 10.1166/jbn.2011.1244
10. Paleos, C. M.; Tsiourvas, D.; Sideratou, Z.; Tziveleka, L. *Biomacromolecules*, **2004**, 5, 524. **DOI:** 10.1021/bm030068h
11. Kisak, E. T.; Coldren, B.; Evans, C. A.; Boyer, C.; Zasadzinski, J. A. *Curr.Med.Chem*. **2004,** *11*, 199. **DOI:** 10.2174/0929867043456197
12. Wu, W.; Wieckowski, G.; Pastorin, M.; Benicasa, M.; Klumpp,C.; Briand, J. P.; Genaro, R.; Prato, M.; Bianco, A. *Angew.Chem,Int.Ed.* **2005**, 44, 6358. **DOI:** 10.1002/anie.200501613
13. Salem, A. K.; Searson, P. C.; Leong, K. W. *Nature Mater*, **2003**, 2, 668. **DOI:** 10.1038/nmat974
14. Paciotti, G. F.; Myer, L.; Weinreich, D.; Goia, D.; Pavel, N.; McLaughlin, R.E.; Tamarkin, L. *Drug Deliv.* **2004**, *11*, 169. **DOI:** 10.1080/10717540490433895
15. Paciotti, G. F.; Kingston, D. G. I.; Tamarkin, L. *Drug Dev Res*, **2007**, *67*, 47. **DOI**: 10.1002/ddr.20066
16. Patra, C. R.; Bhattacharya, R.; Mukhopadhyay, D.; Mukherjee, P. *J. Biomed. Nanotechnol.* **2008**, *4*, 99. **DOI:** 10.1166/jbn.2008.016
17. Rastogi, L.; Arunachalam, J. *Adv. Mat. Lett.* **2013**, *4*, 548 **DOI**: 10.5185/amlett.2012.11456
18. Basavegowda1, N.; Sobczak-Kupiec, A.; Malina, D.; Yathirajan, S. H.; Keerthi V. R.; Chandrashekar, N.; Dinkar, S.; Liny, P. *Adv. Mat. Lett*. **2013,** 4, 332 **DOI:** 10.5185/amlett.2012.9423
19. Rigobello, M.; Folda, A.; Baldoin, M.; Scutari, G.; Bindoli, A. *Free Radical.Res*. **2005**, *39*, 687. **DOI:** 10.1080/10715760500135391
20. Kim, I.; Jin, J.; Lee, I.; Park, S. *Brit. J. Pharm*, **2004**, *142*, 749. **DOI:** 10.1038/sj.bjp.0705708
21. Shaw, C.F.; *Chem.Rev*, **1999**, 99, 2589 **DOI:** 10.1021/cr980431o
22. Han, G.; Ghosh, P.; De, M.; Rotello,V. M. *Nanobiotechnology*, **2007**, *3*, 40. **DOI**: 10.1007/s12030-007-0005-3
23. Hainfeld, J. F.; Slatkin, D. N.; Smilowits, H. M. *Phys. Med. Biol*, **2004**, *49*, N309. **DOI:** 10.1088/0031-9155/49/18/N03
24. Tiwari, A.; *Polysachharides: Development, Properties and Application*, Nova Science Publishers, Inc, New York, USA. **2010**, pp 552. **ISBN:** 978-1-60876-544-7
    Tiwari, A. *Journal of Inorganic and Organometallic Polymers and Materials*, **2009**, *19*, 361.
25. Shukla, S. K.; Deshpande, S. R.; Shukla, S. K.; Tiwari, A.; *Talanta*, **2012**, *99*, 283. **DOI:** 10.1016/j.talanta.2012.05.052
26. Tiwari, A.; Terada, D.; Sharma, P. K.; Parashar, V.; Yoshikawa, C.; Pandey, AC.; Kobayashi, H. *Anal. Methods*, **2011**, *3*, 217. **DOI:** 10.1039/C0AY00574F
27. Gaidhane, M. K.; Rahatgaonkar, A. M.; Tiwari, A.; Chorghade, M .S. *J Inorg Organomet Polym.*, **2011,** *21*,118. **DOI:** 10.1007/s10904-010-9422-1
28. Shukla, S. K.; Tiwari, A.; *Adv. Mater. Res*., **2011**, *82*, 306. **DOI:** 10.4028/www.scientific.net/AMR.306-307.82
29. Cao, S.; Mishra, R.; Pilla, S.; Tripathi, S.; Pandey, M. K.; Shah, G.; Mishra, A. K.; Prabaharan, M.; Mishra, S. B.; Xin, J.; Pandey, R. R.; Wu, R. R.; Pandey, A. C.; Tiwari, A. *Carbohyd.Polym.* **2010**, *82*, 189. **DOI:** 10.1016/j.carbpol.2010.04.051
30. Mouryaa, V. K.; Inamdara, N. N.; Tiwari, A. *Adv. Mater. Lett*., **2010**, *1*, 11 **DOI:** 10.5185/amlett.2010.3108
31. Tiwari, A.; Aryal, S.; Pilla, S.; Gong, S. *Talanta*, **2009,** *78*, 1401. **DOI:** 10.1016/j.talanta.2009.02.038
32. Tiwari, A.; Dhakate, S. R. *Int. J. Biol. Macromol*, **2009**, *44*, 408. **DOI:** 10.1016/j.ijbiomac.2009.03.002
33. Vasconcelos, H. L.; Camargo, T. P.; Goncalves, N. S.; Neves, A.; Laranjeira, M. C. M.; Favere,V. T. *React.Funct.Polym*, **2008**, *68*, 572. **DOI:** 10.1016/j.reactfunctpolym.2007.10.024
34. Yang, T. C.; Li, C. F.; Chou, S. S.; Chou, C. C. *J.Appl.Polym.Sci*, **2005**, *98*, 564. **DOI:** 10.1002/app.21255
35. Huang, H.; Yang, X. *Carbohyd.Res.* **2004**, *339*, 2627. **DOI:** 10.1016/j.carres.2004.08.005
36. Huang, H.; Yuan, Q.; Yang, X. *Colloid Surf B.* **2004**, *39*, 31. **DOI:** 10.1016/j.colsurfb.2004.08.01
37. Huang, H.; Yang, X. *Biomacromolecules.* **2004,** *5*, 2340. **DOI:** 10.1021/bm0497116
38. Ma,Y.; Li, N.; Yang, C.; Yang, X. *Anal. Bioanal. Chem*, **2005**, *382*, 1044. **DOI:** 10.1007/s00216-005-3222-4
39. Bhumkar, D. R.; Joshi, H. M.; Sastry, M.; Pokharkar, V. B. *Pharm. Res*. **2007**, *24*, 1415. **DOI:** 10.1007/s11095-007-9257-9
40. Sosnik, A.; Carcaboso, A. M.; Glisoni, R. J.; Moretton, M. A.; Chiappetta, D. A.; *Adv.Drug Deliv.Rev.* **2010,** *62*, 547. **DOI:** 10.1016/j.addr.2009.11.023
41. Huang, H. Z.; Qiang, Y.; Yang, X. R. *J. Colloid Interface Sci*, **2005**, 282, 26. **DOI:** 10.1016/j.jcis.2004.08.063
42. Wei, D. W.; Qian, W, P. *J.Nanosci.Nanotechnol.* **2006**, *6*, 2508. **DOI:** 10.1166/jnn.2006.530
43. Esumi, K.; Takei, N.; Yoshimura, T. *Colloids Surf., B. Biointerfaces*, **2003**, *32*, 117. **DOI:** 10.1016/S0927-7765(03)00151-6
44. Raveendran, P.; Fu, F.; Wallen, S. L. *Green Chem.* **2006**, *8*, 34. **DOI:** 10.1039/B512540E

45. Liu, J.; Qin, G.; Raveendran, P.; Ikushima, Y. *Chem. Eur. J.* **2005**, *12*, 2131.
DOI: 10.1002/chem.200500925
46. Huang, H.; Yang, X. *Biomacromolecules*, **2004**, *5* , 2340
DOI: 10.1021/bm0497116
47. Newman, J. D. S.; Roberts, J. M.; Blanchard, G. J. *Anal. Chim. Acta*, **2007**, ***602***, 101.
DOI: 10.1016/j.aca.2007.08.051
48. Huang, L.; Zhau, M.; Peng, J.; Li, J.; Wei, G. J. *Colloid Interface Sci*. **2007**, *316*, 398.
DOI: 10.1016/j.jcis.2007.07.039
49. Santos, R. H. T.; Santos, N. G.; Alves, J. P. H.; Garcia, A.B.G.; Romao, L. C. P.; Arguelho, M. L. P. M. *Bioelectrochemistry.* **2008**, *72*, 122.
DOI: 10.1016/j.bioelechem.2008.01.003
50. Thornsberry**,** C.; Hill, B. C.; Swenson J. M.; McDougal, L. K, *Clin Infect Dis.* **1983**, *5*, S412.
DOI: 10.1093/clinids/5.Supplement_3.S412

